Theory and Applications of Coupled Optical Waveguides Involving Anisotropic or Gyrotropic Materials

KENICHI KITAYAMA, MEMBER, IEEE, AND NOBUAKI KUMAGAI, SENIOR MEMBER, IEEE

Abstract—**Coupled optical waveguides consisting of two isotropic dielectric slab waveguides coupled through anisotropic or gyrotropic materials inserted between them, are treated theoretically in detail. The properties of reciprocal and nonreciprocal TE–TM mode conversion and a nonreciprocal phase shift for TM modes are shown. As an example of application of this type of coupled waveguide, a nonreciprocal optical integrated circuit (IC) mode converter is proposed. It is shown that a circulator and an isolator which require neither mode separators nor mode filters can be constructed by utilizing the proposed nonreciprocal mode converter. The numerical design examples are also given.**

I. Introduction

OPTICAL integrated circuits (IC's) with anisotropic or gyrotropic materials are of great interest from both the theoretical and the practical points of view. So far, the electromagnetic wave modes propagating along an anisotropic or gyrotropic slab waveguide have been analyzed by several authors [1]–[3], and various optical IC devices such as mode converter, isolator, circulator, etc., using a waveguide involving an anisotropic or gyrotropic medium have been proposed [4]–[9].

In the present paper, the coupled optical waveguides, consisting of two parallel isotropic dielectric slab waveguides coupled through anisotropic or gyrotropic materials inserted between them, are considered. This is one of the simplest and most typical configurations of the optical IC involving an anisotropic or gyrotropic material. For example, an optical modulator using this type of coupled waveguide has been proposed previously [10]. To the authors' knowledge, however, the detailed analysis of the aforementioned coupled waveguides has not yet been reported so far.

In this paper, the general features of the wave propagation characteristics of this type of coupled waveguide are analyzed theoretically in detail, and the nonreciprocal optical IC mode converter is proposed as an example of application. It is shown that a circulator and an isolator requiring neither mode separators nor mode filters can be constructed utilizing the proposed nonreciprocal mode converter. The numerical design examples are also given.

Manuscript received March 18, 1976; revised November 19, 1976.
K. Kitayama was with the Department of Electrical Communication Engineering, Faculty of Engineering, Osaka University, Suita-shi, 565 Japan. He is now with the Ibaragi Electrical Communication Laboratory, Nippon Telegraph and Telephone Public Corporation, Tokai-mura, Ibaragi, Japan.
N. Kumagai is with the Department of Electrical Communication Engineering, Faculty of Engineering, Osaka University, Suita-shi, 565 Japan.

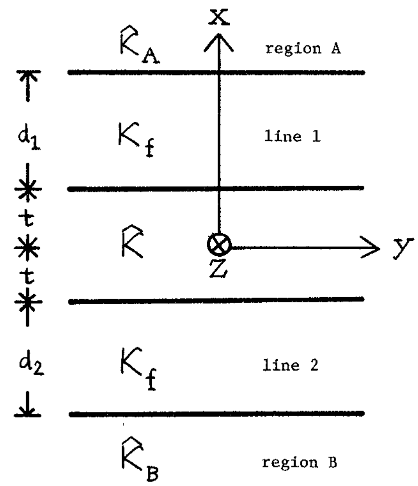

Fig. 1. Geometry of the coupled dielectric slab waveguides coupled through anisotropic or gyrotropic material.

II. Waveguide Configuration and the Basis of Analysis

A. Waveguide Configuration

The coupled waveguide to be considered is a two-dimensional structure, as shown in Fig. 1, being uniform in the y direction. The direction of wave propagation is parallel to the z axis. Lines 1 and 2 are the isotropic dielectric slab waveguides whose permittivity is $\varepsilon_0\kappa_f$ where ε_0 is the permittivity in vacuum. The medium between lines 1 and 2 is anisotropic or gyrotropic with tensor permittivity $\varepsilon_0\hat{\kappa}$. The permittivity tensors $\varepsilon_0\hat{\kappa}_A$ and $\varepsilon_0\hat{\kappa}_B$ in regions A and B, respectively, are assumed to be diagonal. It is assumed that the permeabilities in all regions are equal to the permeability in vacuum μ_0. It is assumed further that the media involved are dissipation free.

The specific permittivity tensor $\hat{\kappa}$ is expressed, in general, in the form

$$\hat{\kappa} = \begin{bmatrix} \kappa_{xx} & \kappa_{xy} & \kappa_{xz} \\ \kappa_{xy}^* & \kappa_{yy} & \kappa_{yz} \\ \kappa_{xz}^* & \kappa_{yz}^* & \kappa_{zz} \end{bmatrix} \tag{1}$$

where the asterisk denotes the complex conjugate. We shall distinguish the *anisotropic* material from the *gyrotropic* material in the following manner: The *anisotropic* material is a matter for which all the off-diagonal terms in $\hat{\kappa}$ are real while the *gyrotropic* material is a matter for which all the off-diagonal terms in $\hat{\kappa}$ are pure imaginary. The diagonal

TABLE I
CLASSIFICATION OF PERTURBED SYSTEMS

	Longitudinal(L)	Polar(P)	Equatorial(E)
$\hat{\kappa}$	$\begin{bmatrix}\kappa_{xx} & \kappa_{xy} & 0\\ \kappa^*_{xy} & \kappa_{yy} & 0\\ 0 & 0 & \kappa_{zz}\end{bmatrix}$	$\begin{bmatrix}\kappa_{xx} & 0 & 0\\ 0 & \kappa_{yy} & \kappa_{yz}\\ 0 & \kappa^*_{yz} & \kappa_{zz}\end{bmatrix}$	$\begin{bmatrix}\kappa_{xx} & 0 & \kappa_{xz}\\ 0 & \kappa_{yy} & 0\\ \kappa^*_{xz} & 0 & \kappa_{zz}\end{bmatrix}$
Anisotropic(A)	A L κ_{xy}, κ^*_{xy}: real	A P κ_{yz}, κ^*_{yz}: real	A E κ_{xz}, κ^*_{xz}: real
Gyrotropic(G)	G L κ_{xy}, κ^*_{xy}: pure imag. (z direction)*	G P κ_{yz}, κ^*_{yz}: pure imag. (x direction)*	G E κ_{xz}, κ^*_{xz}: pure imag. (y direction)*

(* The direction of applied magnetic field).

terms in $\hat{\kappa}$ are real for both anisotropic and gyrotropic media. The anisotropic property can be realized by applying an electric field to the electrooptic materials, or rotating the crystal axis of the optical crystals. The gyrotropic property, on the other hand, can be obtained by applying a magnetic field to the magnetooptic materials.

B. Basis of the Analysis

In most practical cases, the change of the material constants of electrooptic or magnetooptic materials caused by the applied electric or magnetic fields is very small. Therefore, the coupled waveguides system shown in Fig. 1 can be regarded as a slightly perturbed system, perturbed from an unperturbed system which possesses the diagonal permittivity tensor $\varepsilon_0\hat{\kappa}'$ in place of $\varepsilon_0\hat{\kappa}$, where $\hat{\kappa}'$ is given by

$$\hat{\kappa}' = \begin{bmatrix}\kappa_{xx} & 0 & 0\\ 0 & \kappa_{yy} & 0\\ 0 & 0 & \kappa_{zz}\end{bmatrix} \quad \text{(unperturbed).} \qquad (2)$$

The nonzero off-diagonal terms in $\hat{\kappa}$ are thought to appear as a result of slight perturbation caused by the applied electric or magnetic fields. It is assumed that the diagonal terms in $\hat{\kappa}$ and the tensor permittivities $\hat{\kappa}_A$ and $\hat{\kappa}_B$ in regions A and B are not affected by the applied fields.

According to the positions of nonzero off-diagonal terms in $\hat{\kappa}$, the perturbed coupled waveguides system shown in Fig. 1 can be classified in three categories [7]. These are longitudinal (L), polar (P), and equatorial (E) perturbations as shown in Table I. Further, each perturbation is divided into anisotropic (A) and gyrotropic (G) types. Consequently, we have to treat the wave propagation characteristics about the aforementioned six perturbed systems.

Let us consider now two individual basic waveguide systems as shown in Fig. 2(a) and (b). This figure shows the basic configurations of the individual lines 1 and 2. The medium of permittivity tensor $\varepsilon_0\hat{\kappa}'$ extends in the regions of $x \leq t$ and $x \geq -t$ for the basic configurations of the individual lines 1 and 2, respectively. Hereafter, we shall refer to the guided modes propagating in these two individual basic waveguide systems as elementary modes.

Fig. 3 illustrates numerically the propagation constants of the lowest two elementary modes of lines 1 and 2.

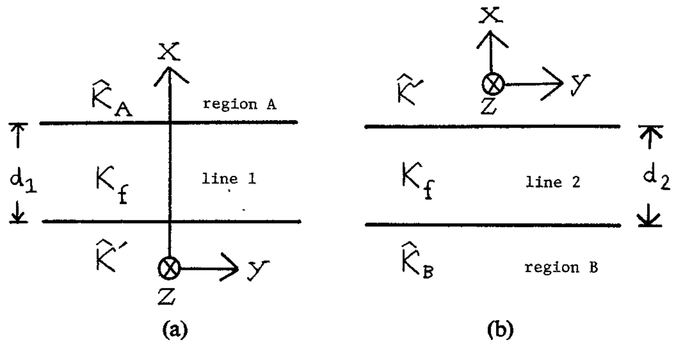

Fig. 2. Geometry of two individual basic lines. (a) The basic configuration of line 1. (b) The basic configuration of line 2.

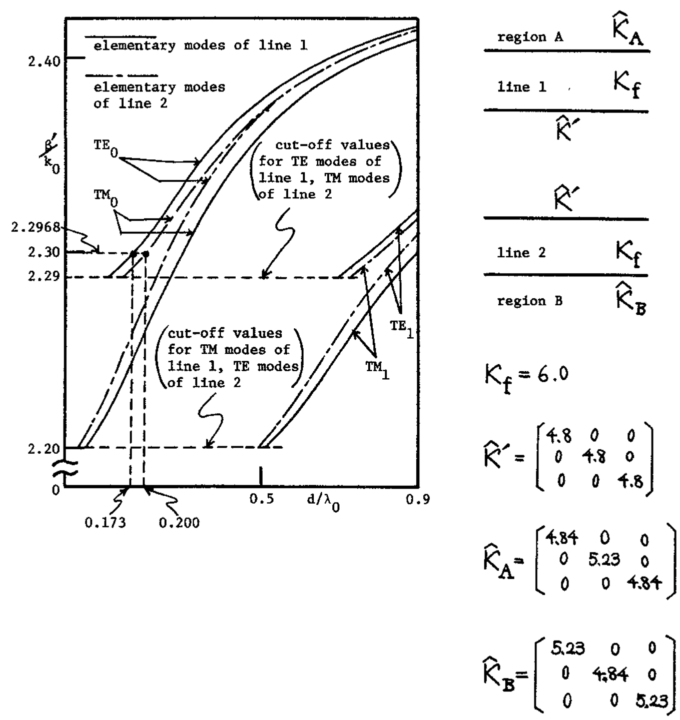

Fig. 3. Dispersion curves for the lowest two elementary modes propagating along each individual basic line.

The values of the permittivities in the regions used in the numerical calculations are shown in the same figure. The values used as a numerical example correspond to the following materials: The slab waveguide consists of As_2S_3[11], the media in regions A and B are TeO_2[12], and the medium between two lines is assumed to be $K_3Li_2Nb_5O_{15}$[13] as an anisotropic material and YIG [6] as a gyrotropic material. Operation wavelength is assumed to be $\lambda_0 \simeq 1.152\,\mu$m. The ordinate is a propagation constant β' normalized by the propagation constant in free space k_0 ($= \omega\sqrt{\varepsilon_0\mu_0}$), and the abscissa is a film thickness d_1, or d_2, of the line 1, or line 2, normalized by a free-space wavelength λ_0 ($= 2\pi/k_0$).

Since the permittivity tensor $\hat{\kappa}'$ is diagonal, TE and TM modes of propagation can be supported in the basic systems. The normalized propagation constant β'/k_0 of the guided modes in a dielectric slab waveguide possesses two limiting values. The upper limit is determined by the refractive index of the film, whereas the lower limit is determined by either one of the refractive indices of the surrounding media whose refractive index is larger than the other. In the case of our numerical example, the lower limits of the normalized propagation constant of the elementary modes in two basic systems are different for the TE modes and the TM modes as we can see from Fig. 3. The TE modes of line 1 are cut off at $\beta'/k_0 = \sqrt{5.23} = 2.29$ while the TM modes at $\beta'/k_0 = \sqrt{4.84} = 2.20$. Similarly, the TE modes of line 2 are cut off at 2.20 and the TM modes at 2.29. By choosing the film thicknesses d_1, d_2 of lines 1 and 2 appropriately, the elementary modes of lines 1 and 2 can be degenerated. The points in Fig. 3 (i.e., $d_1/\lambda_0 = 0.173$ and $d_2/\lambda_0 = 0.200$) show the example of the film thicknesses for which the dominant TE mode (TE_0) of line 1 and the dominant TM mode (TM_0) of line 2 are degenerated.

III. Analysis Based on the Variational Method

A. Normal Mode Analysis of the Perturbed Systems

Since the off-diagonal terms in $\hat{\kappa}$ which appeared as a result of the perturbation are actually very small in most practical cases, the electromagnetic fields of the normal modes propagating along the perturbed systems can be expressed approximately in terms of the linear combinations of the elementary modes of lines 1 and 2.

Let us suppose now that, by choosing the film thicknesses d_1 and d_2 appropriately, the TE_0 mode of line 1 and the TM_0 mode of line 2 are degenerated or nearly degenerated, and the coupling between these two degenerated modes and other modes is small enough to be negligible. Then the field distributions of the normal mode in the perturbed system can be expressed by the linear combinations of the electric and magnetic fields of the elementary modes TE_0 and TM_0. Hence, applying the variational technique given in [14], the sufficiently precise value of the propagation constant and the field distributions of the normal mode in the perturbed systems can be obtained. If the spacing between lines 1 and 2 is very small, or the difference between the refractive indices of the film and the intermedium between the two lines is very small, the accuracy of the aforementioned method of analysis becomes poor. This will be discussed in Section III-B with numerical examples.

Let the normalized complex amplitudes of the TE_0 mode of line 1 and the TM_0 mode of line 2 be $a_1(z)$ and $a_2(z)$, respectively. Then, the complex amplitudes $a_1(z)$ and $a_2(z)$ can be expressed in terms of the complex amplitudes $a_1(0)$ and $a_2(0)$ at the beginning of the coupling portion $z = 0$ as follows:

$$\begin{bmatrix} a_1(z) \\ a_2(z) \end{bmatrix} = [S]^F \begin{bmatrix} a_1(0) \\ a_2(0) \end{bmatrix} [\exp(-j\beta_0 z)] \quad (3)$$

where

$$[S]^F = \begin{bmatrix} S_{11} & S_{12} \\ S_{21} & S_{22} \end{bmatrix} \quad (4)$$

and

$$\beta_0 = (\beta_1 + \beta_2)/2$$

where β_1 and β_2 are the propagation constants of the elementary modes TE_0 and TM_0 of lines 1 and 2, respectively. The matrix $[S]^F$ given by (4) can be regarded as a scattering matrix with respect to the waves propagating in the positive z direction, i.e., the forward waves. We will derive in Section IV-A the scattering matrix which describes the whole system including both forward and backward waves.

L and P Perturbations: The matrix elements in $[S]^F$ are given by

$$\begin{aligned} S_{11} &= \cos cz - j\,\Delta \sin cz \\ S_{12} &= -j(1/\alpha)\sqrt{1-\Delta^2}\sin cz \\ S_{21} &= -j\alpha\sqrt{1-\Delta^2}\sin cz \\ S_{22} &= \cos cz + j\,\Delta \sin cz \end{aligned} \quad (5)$$

where

$$C = \beta_0 F\sqrt{1+(\delta/F)^2} \qquad \delta = (\beta_1 - \beta_2)/(\beta_1 + \beta_2)$$
$$\Delta = (\delta/F)/\sqrt{1+(\delta/F)^2} \qquad F = |N_{12}'|/4\beta_0$$
$$N_{ij}' = \omega\varepsilon_0 \int_{-\infty}^{\infty} e_i \cdot (\hat{\kappa} - \hat{\kappa}')e_j \, dX \qquad (i, j = 1, 2). \quad (6)$$

N_{ij}' is regarded as a perturbation term in which $\boldsymbol{e}_1$ and $\boldsymbol{e}_2$ denote the electric field vectors of the TE_0 mode of line 1 and the TM_0 mode of the line 2, respectively. For each perturbation, the coefficient α in the equations given by (5) becomes as follows:

$$\alpha = \begin{cases} +1, & (N_{12}' > 0) \\ -1, & (N_{12}' < 0) \end{cases} \quad (7)$$

for *AL* and *GP* perturbations, and

$$\alpha = \begin{cases} +j, & (\tilde{N}_{12} > 0) \\ -j, & (\tilde{N}_{12} < 0) \end{cases} \quad (8)$$

for *GL* and *AP* perturbations, where $\tilde{N}_{12}'$ in (8) is a real quantity defined as such $N_{12}' = j\tilde{N}_{12}'$ and $j = \sqrt{-1}$.

GE Perturbation: The scattering matrix defined by (3) becomes diagonal in the form

$$[S]^F = \begin{bmatrix} \exp(-j\delta\beta_0 Z) & 0 \\ 0 & \exp[j(\delta\beta_0 - \Delta\beta_2)Z] \end{bmatrix} \quad (9)$$

where

$$\Delta\beta_2 = N_{22}'/D_{22}. \quad (10)$$

In the case of *L*- and *P*-perturbation systems, the coupling may occur between TE_0 and TM_0 modes since $S_{12} \neq 0$ and $S_{21} \neq 0$ as shown in (5). Further, by comparing *AL* perturbation with *GL* perturbation, it can be seen that the TM_0 mode output is 90° out of phase with respect to the TE_0 mode. Similarly, by comparing *GP* perturbation with *AP* perturbation, we found that the phase of the TE_0 mode output is different in 90° from that of the TM_0 mode.

In the case of *GE* perturbation, no mode conversion between TE_0 and TM_0 modes can be expected, and the TM_0 mode suffers additional phase shift due to the perturbation in the amount of $\Delta\beta_2 z$. *AE* perturbation, on the other hand, causes no influence on both TE_0 and TM_0

modes. We shall omit, therefore, the case of the *AE* perturbation in the following considerations.

In order to discuss the wave propagation characteristics such as, for instance, the nonreciprocal properties of the perturbed systems, the backward waves must be taken into consideration as well as the forward waves.

The scattering matrices $[S]^B$ for the backward waves can be derived by a similar manner as that described in [7]. In the result, for both *AL*- and *GL*- perturbation systems, the scattering matrices $[S]^B$ for the backward waves become entirely the same as $[S]^F$ for the forward waves, while in *P*-perturbation systems, the signs of off-diagonal terms S_{12} and S_{21} are reversed, and in *GE*-perturbation systems, the sign of $\Delta\beta_2$ is reversed.

By comparing the matrices $[S]^B$ with that for the forward waves given by (4) and (9), we find the following features of the wave propagation characteristics of the perturbed systems: The *L*-perturbation systems are bilateral, since the scattering matrices are invariant regardless of the direction of the wave propagation. On the contrary, in the *P*-perturbation systems, the phase shift for the $TM_0(TE_0)$ mode output relative to the $TE_0(TM_0)$ mode input shows 180° difference between forward and backward directions of propagation. In the *EG*-perturbation system, on the other hand, the phase of the TM_0 mode lags by $\Delta\beta_2 z$ in the forward direction, while it leads by $\Delta\beta_2 z$ in the backward direction, both comparing with that in the unperturbed systems.

B. Numerical Example

Fig. 4 illustrates numerically the normalized propagation constants β/k_0 of the normal modes propagating in the forward direction in *L*-, *P*-, and *GE*-perturbation systems. The film thicknesses d_1 and d_2 of line 1 and line 2 were chosen as $d_1/\lambda_0 = 0.173$ and $d_2/\lambda_0 = 0.200$ so that the TE_0 mode of line 1 and TM_0 mode of line 2 are degenerated as shown in Fig. 3. In our example, the TM_0 mode of line 1 and TE_0 mode of line 2 can also be propagated. However, the coupling between these two modes and the aforementioned degenerated TE_0 mode of line 1 and TM_0 mode of line 2 is weak enough to be negligible because the differences of propagation constants between these two mode groups are sufficiently large (about 10^2 times) compared with the perturbation terms as we can see from Fig. 3. It can be shown further that, in our numerical example, the proposed approximate method of analysis using only two elementary modes is certified with satisfactory accuracy as long as the spacing $2t$ between two lines is greater than $\lambda_0/2$ (i.e., $2t/\lambda_0 > 0.5$). However, in order to obtain the sufficiently strong coupling, it is desirable to choose the spacing $2t$ smaller than about $1.5\lambda_0$ (i.e., $2t/\lambda_0 < 1.5$).

We can see from Fig. 4 that the normalized propagation constants of the normal modes in the *L*- and *P*-perturbation systems approach that of the degenerated elementary modes, $\beta_1/k_0 = \beta_2/k_0 = 2.2968$, as increasing the spacing between two lines. In the *GE*-perturbation system, on the other hand, either one of the propagation constants varies in the amount of $\Delta\beta_2$ due to the perturbation.

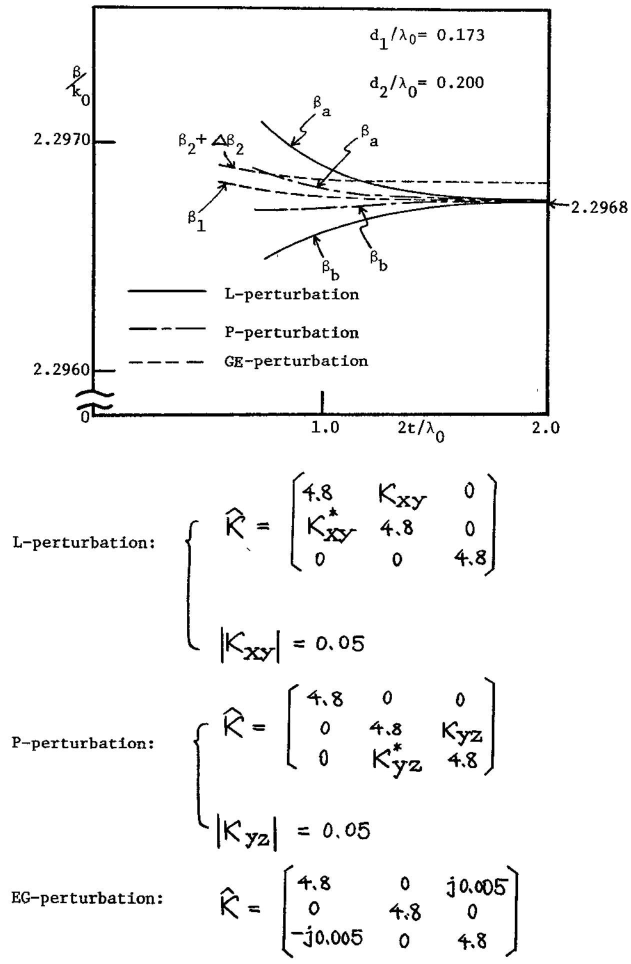

$$\text{L-perturbation: } \hat{K} = \begin{bmatrix} 4.8 & K_{xy} & 0 \\ K_{xy}^* & 4.8 & 0 \\ 0 & 0 & 4.8 \end{bmatrix}, \quad |K_{xy}| = 0.05$$

$$\text{P-perturbation: } \hat{K} = \begin{bmatrix} 4.8 & 0 & 0 \\ 0 & 4.8 & K_{yz} \\ 0 & K_{yz}^* & 4.8 \end{bmatrix}, \quad |K_{yz}| = 0.05$$

$$\text{EG-perturbation: } \hat{K} = \begin{bmatrix} 4.8 & 0 & j0.005 \\ 0 & 4.8 & 0 \\ -j0.005 & 0 & 4.8 \end{bmatrix}$$

Fig. 4. Dispersion curve for forward normal modes of *L*-, *P*-, and *GE*-perturbation systems.

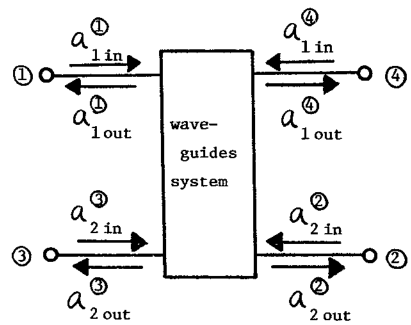

$a^{①}_{1\,in}$, $a^{①}_{1\,out}$, $a^{④}_{1\,in}$, $a^{④}_{1\,out}$, $a^{③}_{2\,in}$, $a^{③}_{2\,out}$, $a^{②}_{2\,in}$, $a^{②}_{2\,out}$

Fig. 5. Circuit-theoretic model for the coupled waveguide system.

IV. Treatment of the Perturbed Waveguide Systems Using a Scattering Matrix

A. Scattering Matrix for the Whole System

Let us take only two degenerated elementary modes into consideration as mentioned in the preceding example. If we assign one port to each input end of particular forward and backward elementary modes, the perturbed waveguide system can be expressed as shown in Fig. 5. The ports ① and ④ denote the input ends of the forward and backward TE_0 mode of line 1, respectively, while the ports ③ and ② represent the input ends of the forward and backward TM_0

mode of line 2, respectively. $a_1(z)$ and $a_2(z)$ are the normalized complex amplitudes of the TE_0 mode of line 1 and TM_0 mode of line 2, respectively. A superscript ⓘ ($i = 1,2,3,4$) denotes the port number, and the subscripts "in" and "out" mean input and output, respectively. The scattering matrix describing the whole system can then be expressed as

$$\boldsymbol{a}_{\text{out}} = \exp(-j\beta_0 l)[S] \cdot \boldsymbol{a}_{\text{in}}$$

$$[S] = \begin{bmatrix} \mathbf{0} & [S]^B \\ [S]^F & \mathbf{0} \end{bmatrix} \tag{11}$$

where $[S]^F$ and $[S]^B$ are the scattering matrices for the forward and backward waves, respectively, obtained in the preceding section, l denotes the length of the system, and

$$\boldsymbol{a}_{\text{out}} = {}^T(a_{1\,\text{out}}^{①}, a_{2\,\text{out}}^{③}, a_{1\,\text{out}}^{④}, a_{2\,\text{out}}^{②})$$

$$\boldsymbol{a}_{\text{in}} = {}^T(a_{1\,\text{in}}^{①}, a_{2\,\text{in}}^{③}, a_{1\,\text{in}}^{④}, a_{2\,\text{in}}^{②})$$

$$\mathbf{0} = \begin{bmatrix} 0 & 0 \\ 0 & 0 \end{bmatrix}. \tag{12}$$

In (12), T denotes the transpose. Since the system is assumed to be dissipation free, the scattering matrix $[S]$ is unitary.

The system is reciprocal provided that the scattering matrix is symmetrical. On the contrary, if

$$[S]^F \neq {}^T[S]^B \tag{13}$$

the system becomes nonreciprocal. The reciprocal and nonreciprocal properties of the perturbed waveguide systems can then be summarized as follows.

L perturbations: The *AL*-perturbation system is reciprocal, but the *GL*-perturbation system is nonreciprocal.

P perturbations: The *AP*-perturbation system is reciprocal, whereas the *GP*-perturbation system is nonreciprocal.

GE perturbation: The *GE*-perturbation system is nonreciprocal.

B. Application to a Nonreciprocal Mode Converter

As stated in the preceding section, the *AL*- and *AP*-perturbation systems show the reciprocal mode conversion while the *GL*- and *GP*-perturbation systems possess the property of nonreciprocal mode conversion, and the *GE*-perturbation system presents the nonreciprocal phase shift.

As an example of application of these perturbed systems, let us consider the nonreciprocal optical IC mode converter consisting of the *GL–AP* combination system as shown in Fig. 6. Again we shall assume that the TE_0 mode of line 1 and the TM_0 mode of line 2 are degenerated. In this case, Δ given by (6) vanishes. Let us designate c in (5) as c_{GL} and c_{AP} for the *GL* and *AP* perturbations, respectively. Let us assume also that the lengths of the *GL*- and *AP*-perturbation systems are so chosen that

$$c_{GL}z = \pi/4 \qquad c_{AP}z = \pi/4. \tag{14}$$

Then, the scattering matrix for the forward wave is yielded by multiplying the matrices for the *GL*- and *AP*-perturbation systems given by (4) as follows:

$$[S]^F = [S]_{AP}{}^F \cdot [S]_{GL}{}^F = \begin{bmatrix} 0 & 1 \\ -1 & 0 \end{bmatrix}. \tag{15}$$

Similarly, the scattering matrix for the backward wave is given by

$$[S]^B = [S]_{GL}{}^B \cdot [S]_{AP}{}^B = \begin{bmatrix} 1 & 0 \\ 0 & 1 \end{bmatrix}. \tag{16}$$

It can be seen from (15) and (16) that this system acts as a circulator rotating the port ① → ② → ③ → ④. Fig. 7 shows the numerical design example of this circulator.

Unlike conventional optical circulators proposed previously, this circulator requires no mode separators at both input and output ports. Furthermore, the line 1 or line 2 of this system can also be utilized as an isolator for the TE_0 mode or the TM_0 mode, respectively, without using the mode filters at both input and output ports.

Besides this example, a wide variety of reciprocal and

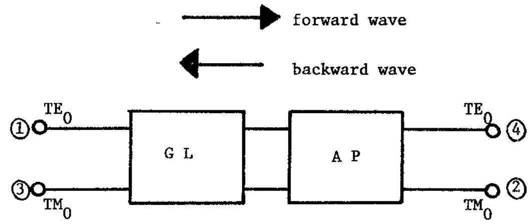

Fig. 6. Nonreciprocal mode converter consisting of *GL–AP* combination system.

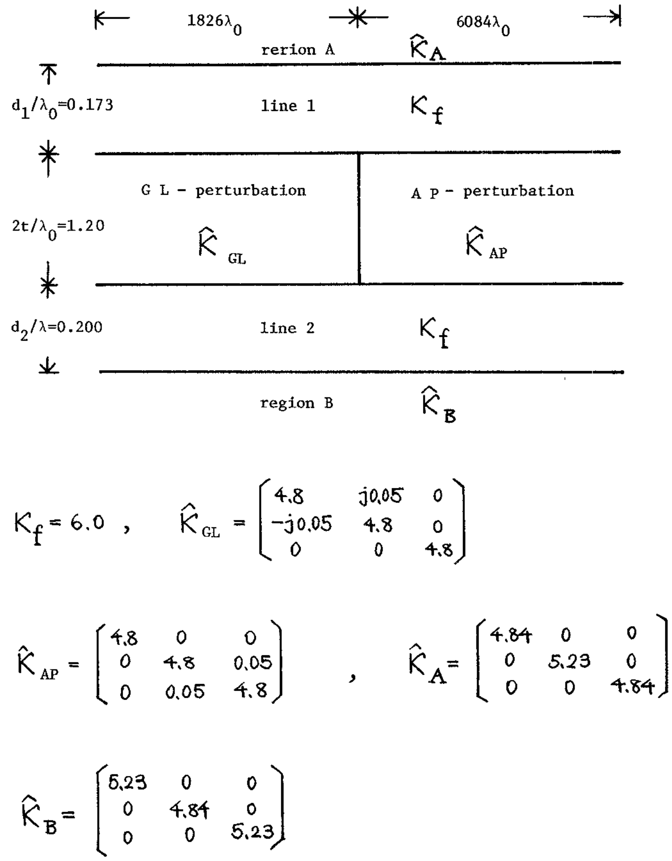

Fig. 7. Numerical design example of circulator using *GL–AP* combination system.

nonreciprocal optical IC devices possessing various functions would be constructed by using the perturbed systems treated in the present paper.

V. Conclusion

The coupled optical waveguides, consisting of two isotropic dielectric slab waveguides coupled through anisotropic or gyrotropic materials inserted between them, have been treated theoretically in detail. It has been found that the *AL*- and *AP*-perturbation systems show the reciprocal mode conversion, while the *GL*- and *GP*-perturbation systems possess the property of nonreciprocal mode conversion, and the *GE*-perturbation system causes nonreciprocal phase shift for the TM_0 mode, whereas the *AE*-perturbation system shows no influence upon both TE_0 and TM_0 modes. As an example of application of these perturbed systems, the nonreciprocal optical IC mode converter has been proposed, and the numerical design example of the optical IC circulator has been given. This circulator requires no mode separators at both input and output ports. This circulator can also be utilized as an isolator without using mode filters at both input and output ports. In order to realize these devices, the progress of the fabrication techniques, together with the development of magnetooptic materials which possess a large Faraday effect, is required.

Acknowledgment

The authors wish to thank Prof. M. Matsuhara and K. Morishita for their useful and stimulative discussions.

References

[1] D. F. Nelson and J. McKenna, "Electromagnetic modes of anisotropic dielectric waveguides at p-n junctions," *J. Appl. Phys.*, vol. 38, pp. 4057–4074, Sept. 1967.
[2] S. Yamamoto, Y. Koyamada, and T. Makimoto, "Normal-mode analysis of anisotropic and gyrotropic thin-film waveguides for integrated optics," *J. Appl. Phys.*, vol. 43, pp. 5090–5097, Dec. 1972.
[3] Y. Satomura, M. Matsuhara, and N. Kumagai, "Analysis of electromagnetic-wave modes in anisotropic slab waveguide," *IEEE Trans. Microwave Theory Tech.*, vol. MTT-22, pp. 86–92, Feb. 1974.
[4] S. Wang, M. Shah, and J. D. Crow, "Studies of the use of gyrotropic and anisotropic materials for mode conversion in thin-film optical-waveguide applications," *J. Appl. Phys.*, vol. 43, pp. 1861–1875, Apr. 1972.
[5] J. Warner, "Faraday optical isolator/gyrator design in planar dielectric waveguide form," *IEEE Trans. Microwave Theory Tech.*, vol. MTT-21, pp. 769–775, Dec. 1973.
[6] J. Warner, "Nonreciprocal magnetooptic waveguides," *IEEE Trans. Microwave Theory Tech.*, vol. MTT-23, pp. 70–78, Jan. 1975.
[7] S. Yamamoto and T. Makimoto, "Circuit theory for a class of anisotropic and gyrotropic thin-film optical waveguides and design of nonreciprocal devices for integrated optics," *J. Appl. Phys.*, vol. 45, pp. 882–888, Feb. 1974.
[8] F. Auracher and H. H. Whitte, "A new design for an integrated optical isolator," *Opt. Com.*, vol. 13, pp. 435–438, Apr. 1975.
[9] S. Yamamoto, Y. Okamoto, and T. Makimoto, "One-section design of composite-type nonreciprocal thin-film optical devices," *Trans. IECE Japan*, vol. 58-C, pp. 491–492, Aug. 1975.
[10] S. Kurazono, K. Iwasaki, and N. Kumagai, "A new optical modulator consisting of coupled optical waveguides," *Trans. IECE Japan*, vol. 55-C, pp. 61–67, Jan. 1972.
[11] L. Bornstein, *Physical Tables*, vol. 2, part 8. Berlin, Germany: Springer, 1962, pp. 2–427.
[12] N. Uchida, "Optical properties of single-crystal paratellurite," *Phys. Rev. B.*, vol. 4, pp. 3736–3745, Nov. 1971.
[13] L. G. Van Uitert, S. Singh, H. J. Levinstein, J. E. Geusic, and W. A. Bonner, "A new and stable nonlinear optical material," *Appl. Phys. Lett.*, vol. 11, pp. 161–163, Sept. 1967.
[14] M. Matsuhara and N. Kumagai, "Theory of coupled open transmission lines and its applications," *IEEE Trans. Microwave Theory Tech.*, vol. MTT-22, pp. 378–382, Apr. 1974.

Linear Power Responses of an Optical Fiber

CHARLES VASSALLO

***Abstract*—It is known that an optical fiber behaves linearly in terms of power when the modulation frequency is smaller than the spectrum width of the light source. In order to calculate the impulse or frequency power responses with a modal calculation, it is shown that the powers carried by the different modes are independent in usual cases. Different formulas are proposed for the linear responses when there is no mode coupling, and the corresponding validity conditions are given.**

I. Introduction

A DESIRABLE characteristic of any transmission system is the linear relation between the output and input variables. In the case of transmission through optical fibers, the output variable is the current generated by the photodetector, and it is proportional to the optical power. Then the fiber must be linear in terms of power. Some aspects of this linearity have already been studied [1], [2]. It may be obtained by using an incoherent source of spectral width $\Delta\nu$ when the modulation frequencies are quite lower than $\Delta\nu$ [1].

A modal calculation of the impulse and frequency power responses, when there is no mode coupling, is proposed (Section III). But before exposing our results, we must justify the validity of such a method (Section II).

II. Do Different Modes Carry Independent Contributions to the Guided Power?

It is commonly assumed that the answer is positive.

Since powers of unmodulated modes are independent in case of lossless guides only, we shall consider our fiber as a

Manuscript received August 30, 1976; revised November 5, 1976.
The author is with the Centre Nacional d'Études des Télécommunications, 22301 Lannion, France.